2022

What Can Hydrography Between the New England Slope, Bermuda and Africa Tell us About the Strength of the AMOC Over the Last 90 years?

T. Rossby

Jaime B. Palter

Kathleen A. Donohue

What Can Hydrography Between the New England Slope, Bermuda and Africa Tell us About the Strength of the AMOC Over the Last 90 years?

What Can Hydrography Between the New England Slope, Bermuda and Africa Tell us About the Strength of the AMOC Over the Last 90 years?

T. Rossby[1] , **J. Palter[1]** , and **K. Donohue[1]**

[1]Graduate School of Oceanography, University of Rhode Island, Kingston, RI, USA

Abstract The Gulf Stream is the only pathway in the subtropical North Atlantic by which warm water flows poleward. This transport of warm water and return of cold water at depth is called the Atlantic Meridional Overturning Circulation (AMOC). The dynamic method is applied to hydrocasts collected since the 1930s to estimate upper-ocean transport (0–1,000 m) between the U.S. Continental Slope and Bermuda and separately to Africa with focus on the longest directly observable timescale. Calculating transport between the Slope and Bermuda eliminates the Gulf Stream's northern and southern recirculation gyres, while calculations between the Slope and Africa remove all other recirculating geostrophic flow. The net Slope-Bermuda upper-ocean transport is estimated to be 41.1 ± 0.4 Sv, decreasing by 2.0 ± 0.8 Sv between 1930 and 2020. The AMOC contribution is 18.4 ± 0.6 Sv, decreasing by 0.4 ± 0.6 Sv between 1930 and 2020.

Plain Language Summary The Gulf Stream is the only pathway by which the ocean transports warm water to high latitudes in the North Atlantic and Nordic Seas where it cools, sinks and flows back south at intermediate depths from the subpolar North Atlantic and at greater depths from the Nordic Seas. This circulation pattern, the Atlantic Meridional Overturning Circulation (AMOC), plays an important role in Earth's climate. But the Gulf Stream is also the wester boundary current to the horizontal circulation driven by the trade winds and westerlies at low and mid-latitudes. The Gulf Stream also drives large recirculations to its south and north. In this study we use hydrographic data taken since the 1930s to calculate the poleward flow in the Gulf Stream, while canceling out the recirculation and wind-driven transports to estimate the strength of the north-flowing portion of the AMOC. There is evidence for a 2.0 Sv Gulf Stream slow-down between 1930 and 2020. Whether and to what extent this reflects a slowdown of the AMOC or wind-driven circulation cannot be established with certainty. Our estimate of a 0.4 Sv AMOC decrease is reported with low confidence.

1. Introduction

The Gulf Stream occupies a central role in Earth's climate, especially for the regions around the North Atlantic (IPCC, 2021; Palter, 2015). The upper poleward branch of the Atlantic Meridional Overturning Circulation (AMOC) is embedded within the Gulf Stream since elsewhere in the subtropical gyre the mean flow is equatorward (e.g., Colin de Verdière et al., 2019). Thus, a change in warm water transport by the Gulf Stream may be an indication that the embedded AMOC is changing too. Climate models project a slowdown in the AMOC due to anthropogenic climate change, which alters the temperature and salinity of the water masses that feed the dense limb of the circulation (Fox-Kemper et al., 2021). Yet, the longest record of direct observations of the AMOC started in 2004 (Cunningham et al., 2007), so it has been challenging to evaluate whether an AMOC decline may have already begun.

Two studies, focused specifically on the Gulf Stream, found no evidence of a trend in Gulf Stream transport over the observational record. The first, Sato and Rossby (SR, 1995) used hydrographic data collected from the 1930s to 1990s relying on the dynamic method to determine transport. The more recent Rossby et al. (2019) used 25 years of directly measured surface and upper ocean velocities. On the other hand, studies using US east coast tide gauge data in an attempt to reconstruct Gulf Stream trends via geostrophy (e.g., Ezer & Dangendorf, 2020; Yin and Goddard, 2013) have concluded that a slowdown was likely over the 20th century. However, Piecuch et al. (2018) showed that the motion of the Earth's crust and redistribution of ice and water played a larger-than-expected role in the 20th century sea level trends, thereby decreasing how much of the tide gauge trend should be attributed to ocean circulation. Armed with techniques to better identify the large-scale geostrophic signal in tide gauge data, Piecuch (2020) reconstructed the Florida Current over the last century
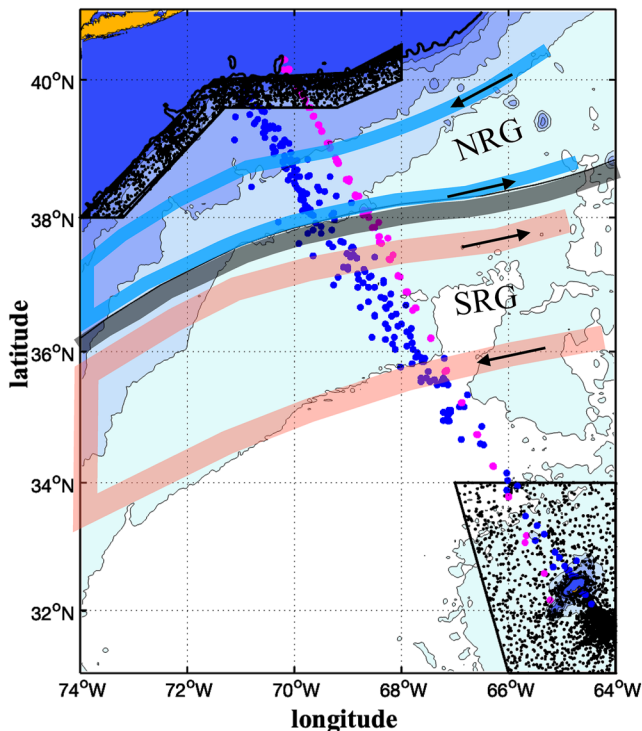
Figure 1. Map of NW Atlantic showing the Slope and Bermuda polygons and hydrographic cast locations. The blue and magenta dots represent the 1930s Atlantis/Iselin and 2010s Line W sections. Black dots indicate other casts. The dark gray band represents the mean Gulf Stream path (from Bisagni et al. (2017)) and the light blue and red bands indicate the northern and southern recirculation gyres (NRG and SRG, resp.). Bathy contours at 200 (thick), 1,000, 2,000, 3,000, 4,000, 5,000 m.

and showed a likely slowdown. Independently, papers have also appeared in recent years suggesting that the AMOC is weakening on decadal and longer time scales (Caesar et al., 2018, 2021), based on a sea surface temperature fingerprint that correlates with AMOC in models, although the ability of this fingerprint to estimate AMOC variations has recently come into question (e.g., Little et al., 2020; Menary et al., 2020; Kilbourne et al., 2022). These studies vary in approach but underscore the controversy surrounding the question of whether the AMOC has slowed over the last century.

This study will revisit the question of AMOC strength using hydrography from the last century with two distinctions from previous studies. First, the analysis will focus on the top 1,000 m to capture all the warm water flowing north in the AMOC since this is the transition depth from poleward to equatorward flow in the subtropics (Danabasoglu et al., 2014; Rossby et al., 2019). This simplifies our task considerably since we need not address the various pathways by which the deep AMOC flows south. We estimate upper ocean transport three ways. First, between the continental slope and Bermuda. This allows us to remove the component of Gulf Stream flow that is associated with the northern and southern recirculation gyres (cf., Ollitrault & Colin de Verdière, 2014). The former is trapped between the Gulf Stream and the continental slope and the latter is confined to latitudes north of Bermuda. What remains are (a) the upper limb of the AMOC, and (b) the wind-driven western boundary current. Second, we estimate the strength of the southward flow between Bermuda and Africa; accounting for this transport allows us to remove all recirculating contributions to the flow between the continental slope and Bermuda and provides one measure of the upper limb of the AMOC alone. Third, we estimate the AMOC directly as the net upper ocean flow north between the continental slope and Africa.

In Section 2, we present the hydrographic data sets used in this study, which will benefit from the extraordinary efforts of Columbus O'D. Iselin in the 1930s. These high-quality sections from Long Island to Bermuda provide the means for assessing long-term change in the AMOC. In Section 3, we describe the methodology that relies heavily upon the well-established dynamic method. Section 4 documents the changes seen since the 1930s. Section 5 presents a summary and discussion.

2. Hydrographic Data

With the start-up of the Woods Hole Oceanographic Institution in 1930, Columbus O'D. Iselin began a program to survey northwest Atlantic waters and the Gulf Stream in considerable detail. The first comprehensive western North Atlantic hydrographic survey was published by Iselin (1936). It was followed soon after with study of Gulf Stream transport variability comprising 15 complete sections between Long Island and Bermuda on a roughly bi-monthly schedule evenly distributed throughout the year (Iselin, 1940). These high quality hydrocasts, with temperature measured to an accuracy of ±0.02°C and ±0.02 ppt (Sverdrup et al., 1942) form a valuable source of information on the state of the Gulf Stream and surrounding waters in the 1930s and were the basis for initiating this study. See Text S1 in Supporting Information S1 for a further discussion of hydrographic measurements.

Two contemporary programs provide invaluable time series: Line W project (1994–2014) took numerous hydrographic sections from the continental slope south toward Bermuda (Andres et al., 2020) and Station S at Bermuda comprises hydrographic stations taken roughly every two weeks since 1954 (e.g., Curry & McCartney, 2001; Joyce & Robbins, 1996). All of these data sources, along with profiles collected by the global Argo program, were downloaded from the Met Office Hadley Centre EN4 database.

Figure 1 shows the Slope Sea and Bermuda polygons that enclose the hydrographic casts used here. The northern polygon is designed to capture hydrographic stations over the continental slope on the far side of the northern recirculation gyre as well as to avoid meanders and warm core rings that could bias the results. This polygon,
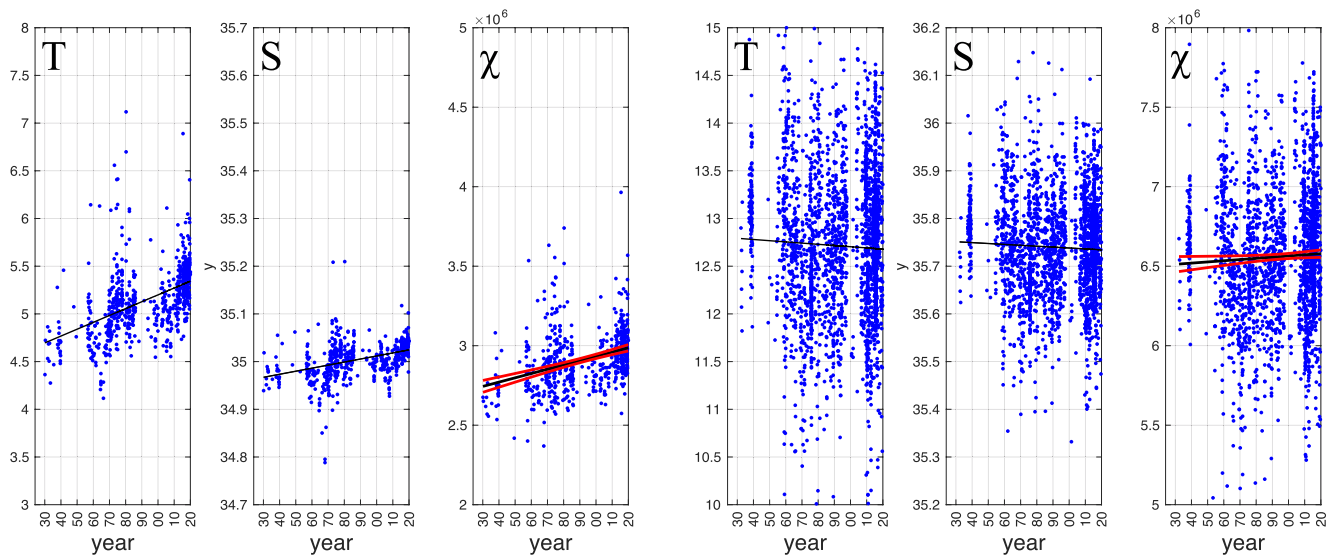
Figure 2. The left and right three panels show 400–1,000 m average temperature, salinity, and 0–1,000 dbar χ for Slope and Bermuda respectively.

which includes 647 casts for this study, will be referred to as the Slope. The southern box with 2,460 casts is composed of the full hydrographic record near Bermuda, including the Station S hydrocasts as well as the above-mentioned Iselin sections from the 1930s with casts inside the box. The left 2 panels in Figure 2 show average temperature and salinity between 400 and 1,000 dbars for Slope and Bermuda respectively. We chose this depth range to emphasize action in the main thermocline and deemphasize seasonal variations which will have little effect as discussed below. For completeness Figures F1 and F2 in Supporting Information S1 show average density in the 3rd subpanels.

We use all historical hydrography and delayed-mode Argo profiles in the EN4 database just west of West Africa, Figure 3, to determine geostrophic transport in the subtropical North Atlantic between Bermuda and Africa, as well as profiles east and west of the Tail of the Grand Banks (TGB) to investigate sources of water-mass changes found along the Slope.
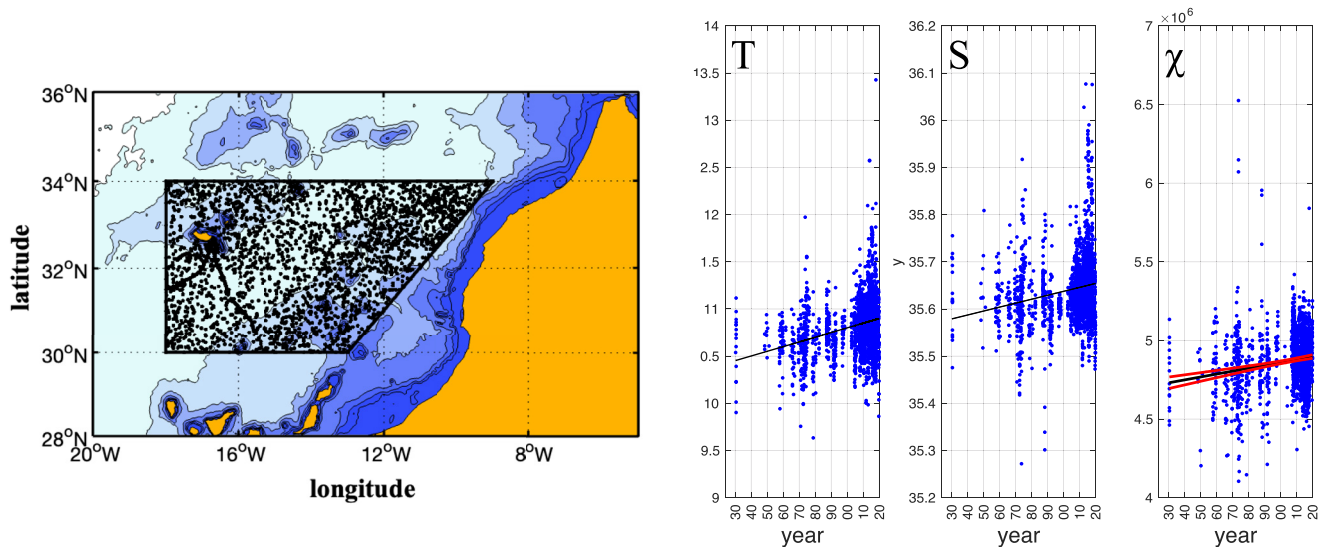

Figure 3. The left panel shows the polygon of hydrographic data just west of Africa used here. The right panel shows 400–1,000 m average temperature, salinity, and 0–1,000 dbar χ.

3. Approach

3.1. Methodology—Potential Energy Anomaly (PEA)

The dynamic method of estimating currents and transport was firmly established over a century ago (e.g., Helland-Hansen & Nansen, 1909). The PEA method of implementing of the dynamic method (UNESCO, 1991) is described below and was first derived by Fofonoff (1962). It is also discussed in some detail in SR from which the following is taken. The key dynamical statement is that geostrophic mass transport (M) can be determined from:

$$M = (\chi_2 - \chi_1) / f,$$

where f is the Coriolis parameter and χ, the PEA, is estimated from two hydrographic profiles bracketing the flow of interest:

$$\chi = 1/g \int_{p_0}^{p} \delta p \, dp.$$

Here δ is the specific volume anomaly, *g is the gravitational constant*, and p is pressure, p_0 is reference pressure, in this case the surface, $p_0 = 0$. The key assumption is that the flow is in geostrophic balance, that is, a steady flow where the pressure gradient force is balanced by the Coriolis acceleration term in the horizontal momentum equation. The appeal of geostrophy is that it captures all flow between two points without needing to know the details between endpoints. Estimating transport from χ is equivalent to estimating the geostrophic velocity from the dynamic height anomaly difference ΔD between two hydrocasts and then integrating to get transport. Note that the χ integral is identical to the dynamic height anomaly integral:

$$\Delta D = \int_{p_0}^{p} \delta \, dp$$

except that it also has the factor p, which acts as a weighting factor on δ, such that δ differences at high p have a greater impact on transport than at the surface and in effect this reduces seasonal effects on transport. Here, rather than using sites bracketing the Gulf Stream as in SR which included not only the AMOC, but also the wind-driven western boundary flow and entrained recirculating waters, we examine the difference in χ between the continental slope and Bermuda to remove the transports associated with the recirculation gyres. Hydrographic casts were taken at all times of the year. We do not remove seasonality as multiplication by p in the χ integral deemphasizes variability at the surface (SR). See Text S2 in Supporting Information S1 for further details. We integrate from the surface to $p = 1,000$ dbars where the AMOC stream function reaches its maximum. Transports and associated errors are calculated using the results from simple linear regressions between χ and time. Errors are propagated from the regressions assuming normal distributions.

4. Results

4.1. Estimating the Level of Zero Transport

Our application of the dynamic method depends upon establishing a level of zero average speed. Thanks to the 25-year Oleander program (Rossby et al., 2019), we know from over 700 complete sections of acoustic Doppler current profiler (ADCP)-measured upper ocean currents that the geostrophic sea level difference between Slope and Bermuda is 0.74 ± 0.013 dyn m (not shown). We can then ask at what depth we should put a level of zero transport so that the difference in ΔD, $\delta\Delta D$, equals this at the surface. The ΔD integrals computed using potential density from the surface to 900, 1,000, 1,100 dbars at Slope and Bermuda result in $\delta\Delta D = 0.70$, 0.74, and 0.76 dyn m suggesting a zero level close to 1,000 dbars. An independent, albeit limited, velocity data set was obtained by the cruise vessel Explorer of the Seas equipped with a 38 kHz ADCP that could measure currents to >1,000 m depth. The transport to the depth of zero average speed between 900 and 1,000 m depth was 38 Sv (see Figure 8 in Rossby et al. (2019)). The corresponding sea level difference was 0.7 m. This lower sea level difference is consistent with the fact that average surface transport during this 2006–2010 period was less than the long-term average. The Oleander and Explorer of the Seas results agree within the overlapping observing period (see Text S3 in Supporting Information S1 for further details).

Table 1
Table of PEA at Slope, Bermuda and Africa, Transport and Transport Changes

	χ at 2020 (10^6 J m^{-2})	χ change (yr^{-1}) (1930–2020)	Transport 2020 (Sv)	Transport change (1930–2020)
Slope	3.0 ± 0.02	0.27 ± 0.06	–	–
Bermuda	6.6 ± 0.02	0.07 ± 0.07	–	–
Africa	4.8 ± 0.01	0.21 ± 0.04	–	–
Slope–Bermuda (SB)	–	–	41.1 ± 0.4	−2.0 ± 0.8
Bermuda–Africa (BA)	–	–	−22.7 ± 0.4	1.6 ± 0.8
Slope–Africa	–	–	21.7 ± 0.3	−0.6 ± 0.6
Sum (SB + BA)	–	–	18.4 ± 0.6	−0.4 ± 0.6

4.2. Estimating Transport

The net mass transport between the Slope and Bermuda is determined from the difference (χ_{Bermuda}–χ_{Slope}) integrated to 1,000 dbars and divided by the Coriolis parameter at 37°N, the latitude of maximum velocities and transport. Text S4 discusses this choice of latitude. A linear regression to χ_{Slope} and to χ_{Bermuda} (third subpanels in Figure 2) yields $3.0 ± 0.02 × 10^6$ and $6.6 ± 0.02 × 10^6$ J m^{-2} at year 2020 with trends between 1930 and 2020 of $0.27 ± 0.06 × 10^4$ and $0.07 ± 0.07 × 10^4$ J m^{-2} year^{-1}, respectively (see Table 1). The corresponding transport between the Slope and Bermuda equals $41.1 ± 0.4$ Sv (1 Sverdrup = 10^9 kg s^{-1}) at present, where the uncertainty is almost completely dominated by the 95% confidence limits to the χ_{Slope} fit (red lines). This represents the net poleward transport between Slope and Bermuda based on a linear fit to the last 90 years.

To separate the recirculating geostrophic gyre component of the northward transport from the AMOC, we extend our geostrophic coverage of upper ocean circulation from Bermuda to the African margin. We take the same PEA approach using 1834 profiles in a box bounded 30°–34°N and 10°–18°W, Figure 3. The region chosen is a compromise between including as many casts as possible while still being representative of the eastern margin waters, even though very few casts are available prior to World War 2. The extensive Argo data reveal a weak zonal gradient of χ_{Africa} across the polygon. We use this gradient to project all χ onto a common point at 32°N, 12°W. Ekman transport is negligible between Bermuda and Africa at 32°N (see Text S5 in Supporting Information S1).

We further postulate that if the depth of zero layer transport is at 1,000 dbars for the Oleander line, then the same should be approximately true between Bermuda and Africa since the wind-driven gyre dominates the upper ocean baroclinic field with little or no remaining circulation at 1,000 dbars. The exact choice of depth is not critical as the vertical shear is quite small at these depths (Rossby et al., 2019; Wunsch, 2011). Any uncertainty here will affect the AMOC estimate but will have little impact on the trend which is dominated by the trend in χ at Slope and Africa (next section). The difference, χ_{Africa}–χ_{Bermuda}, divided by the Coriolis parameter is $−22.7 ± 0.4$ Sv transport to the south. Subtracting $22.7 ± 0.4$ Sv from the $41.1 ± 0.4$ Sv total flowing poleward between Slope and Bermuda produces $18.4 ± 0.6$ Sv as our estimate of the AMOC for year 2020. This is slightly larger than, but within the uncertainty, of the $16.9 ± 1.8$ Sv calculated from the RAPID data at 26°N (average ±1 standard deviation of 16 annual means between April 2004 to March 2020, from Frajka-Williams et al. (2021)), but close to the $18 ± 2.5$ Sv at 24°N calculated using inverse methods from a 1992 hydrographic section (Lumpkin and Speer, 2007).

4.3. Estimating AMOC Trend

The increase in temperature and salinity at Slope results in a decrease in density and an increase in χ_{Slope}, because temperature changes contribute more to the density changes than salinity changes (Figure 2, left panels, and Figure F1 in Supporting Information S1). At Bermuda, a very weak, not significant positive trend in χ_{Bermuda} can be discerned even though the 400–1,000 dbar average temperature and salinity are constant (Figure 2, right panels, and Figure F1 in Supporting Information S1). The weak χ_{Bermuda} trend results from warming of the upper ocean in and above what used to be called 18°C water, which is now closer to 19°C (Curry & McCartney, 2001; Stevens et al., 2020). The rate of change in χ_{Slope} in Figure 2 gives us the 1930–2020 change in Slope-Bermuda

transport of -2.0 ± 0.8 Sv. This includes change from both the vertically overturning AMOC and the western boundary flow of the interior geostrophic circulation, what is often referred to as the Sverdrup gyre.

Estimating the trend of the interior geostrophic circulation has been challenged by the limited amount of data prior to World War 2. The trend in χ_{Africa} results in a 1930–2020 slowdown of 1.6 ± 0.8 Sv in the southward interior geostrophic transport where large uncertainty stems from the variance at Bermuda. Subtracting this decrease from Slope-Bermuda trend yields -0.4 ± 1.0 Sv over 1930–2020 as our estimated AMOC change where the uncertainty is added in quadrature from the stated uncertainty of each trend, which means the variance at Bermuda is counted twice.

4.4. Estimating AMOC and Its Trend From Africa-Slope Bypassing Bermuda

We can apply the same PEA methodology to $\chi_{Africa}-\chi_{Slope}$ to estimate the AMOC directly given that the horizontal geostrophic circulation cancels out. In this case AMOC = 21.2 ± 0.3 Sv. The reason for slightly larger transport than that calculated from $(\chi_{Bermuda}-\chi_{Slope})-(\chi_{Africa}-\chi_{Bermuda})$ of 18.4 Sv is that using f (37°N) along this long oblique section implicitly reduces the estimated interior flow for the long subtropical portion of the section and thus overemphasizes the AMOC. The corresponding trend becomes -0.6 ± 0.6 Sv. Estimating trend from $(\chi_{Bermuda}-\chi_{Slope})-(\chi_{Africa}-\chi_{Bermuda})$ excluding the Bermuda variance, which was counted twice, gives us instead -0.4 ± 0.6 Sv decrease over the last 90 years. This is shown in Table 1.

5. Discussion and Summary

The main advance of this note has been to use hydrography to evaluate the trends in the AMOC on the longest directly observable timescale, close to a century, made possible by the high-quality hydrographic surveys and repeat sections taken by C. O'D. Iselin in the 1930s. The direct velocity measurements along the Oleander line confirm a level of zero transport at 1,000 dbars. This is the starting point for this analysis, which is anchored on the premise that the AMOC stream function has its maximum at this depth. This allows us to apply the PEA method to all available hydrographic data to estimate transport. The Bermuda record, which has documented decadal variability but very little long-term trend, suggests little change in the subtropics. The increase in χ_{Africa} results in a decrease in southward transport across 32°N over time. While there is seasonal variability in the region near Africa (Chidichimo et al., 2010), it is limited to the upper ocean such that its impact on the χ_{Africa} estimate is substantially smaller than the mesoscale variability (see Text S1 in Supporting Information S1). The positive trend in χ_{Africa}, greater than that of Bermuda, indicates baroclinic transport east of Bermuda relative to 1,000 dbars of 22.7 Sv to the south that has weakened at 1.6 ± 0.8 Sv from 1930 to 2020.

The result of this study suggests a weakening of the northward, upper-1,000 m transport between the U.S. Continental Slope and Bermuda, that is, the Gulf Stream, of -2 ± 0.8 Sv between 1930 and 2020. Of this 2 Sv slowdown, about 30% is likely attributable to an AMOC decline (i.e., 0.6 ± 0.6 Sv), with the remainder due to a slowdown in the recirculating component of the subtropical circulation. This direct estimate of Gulf Stream and AMOC trends can serve as a reference for two recent studies that show similar long-term trends. Piecuch (2020) infers a likely weakening of the Florida Current of -1.7 ± 3.7 Sv century^{-1} during 1909–2018 based on sea level measurements. The inference in that work is that the upper limb of the AMOC is embedded within the ~32 Sv Florida Current. Further, Piecuch (2020) attempts to separate the AMOC and wind-driven components of the diagnosed Gulf Stream slowdown, using two reanalysis wind products (Compo et al., 2011; Poli et al., 2016). However, the uncertainties were too great to be conclusive, as the two wind products produce trends in the wind-driven transport at the latitude of Bermuda (32°N) of similar magnitude but opposite sign (see Figure 6 in Piecuch (2020)). The total Sverdrup transport across 32°N from the wind products are about −27 and −22 Sv, respectively.

Caesar et al. (2018) argue that an AMOC weakening associated with observed cooling in the subpolar North Atlantic and warming of the Gulf Stream (including its increased influence on the slope) are signatures of the slow-down. They use an ensemble of model simulations from the CMIP5 project to obtain a calibration factor for AMOC change given trends in subpolar sea surface temperature. From the observed cooling they infer a 3 ± 1 Sv decrease in the AMOC over the last 150 years. In this context we should mention the recent paper by Fraser and Cunningham (2021). Using a Bernoulli Inverse approach applied to reanalyzed hydrographic data (EN4) they find no trend to the AMOC over the last 120 years, but they do find a similar decrease as Caesar et al. (2018)
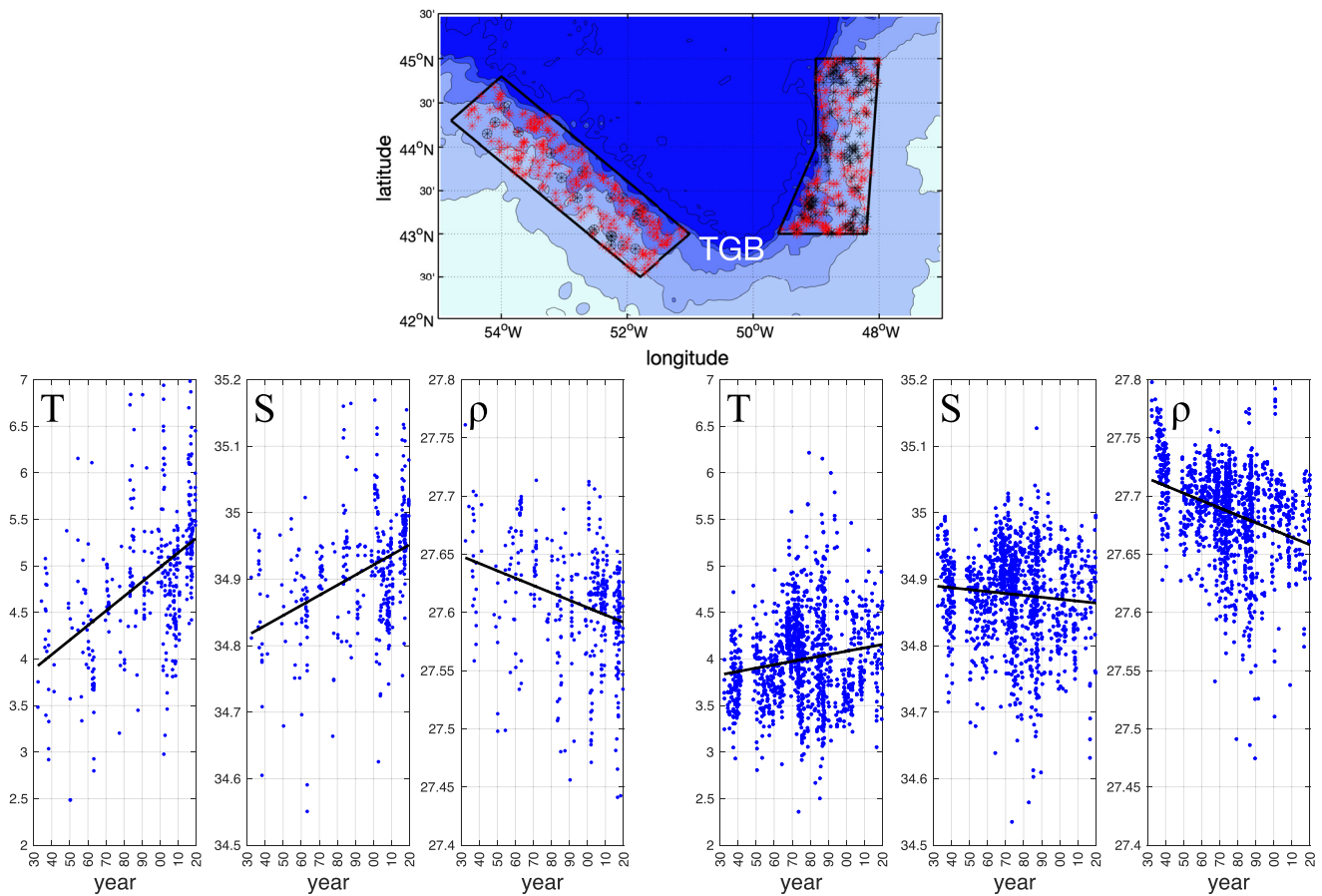
Figure 4. Black and red markers in the two polygons represent casts from the 1930s and 2010s. The left and right three panels below show 300–900 m average temperature, salinity, and density for all casts in the polygons west and east of the TGB, respectively.

since the 1930s. The uncertainty increases in the earliest, and most data-sparse, years of the record, challenging the conclusive exclusion of a long-term trend. Regardless, their work serves as a strong reminder that the trend we report here applies only to the observed period.

The increase in temperature and salinity at Slope has its origins at the TGB. Gonçalves Neto et al. (2021) showed that the conspicuous long-term 0.5°C warming and increased salinity on the northwest Atlantic Shelf since the 1930s can be explained by circulation changes at the TGB. They showed that when the Gulf Stream or its associated eddies come closer to the TGB, they appear to block the Labrador Current from making its sharp westward turn to supply the slope with cool, fresh water. With the Labrador Current increasingly blocked, Gulf Stream waters comprise a higher proportion of the water column along the Slope and Shelf. To illustrate this, we examine water properties in two slope polygons west and east of the TGB, Figure 4. The increasing temperature and salinity to the west—but not east—of the Grand Banks is strong evidence that the property changes seen at Slope must reflect increased contact with the Gulf Stream. This increased contact of the Gulf Stream and Labrador Current may reflect a reduced flow south on the eastern side of the Grand Banks enabling the Gulf Stream to come closer to the TGB. This mechanism appears to be in play in a high-resolution climate model, in which a weakening of Labrador Sea Water formation creates weak anomalies of equatorward transport of dense water along the western subpolar gyre and an AMOC decline after a several-year lag (Yeager et al., 2021).

The transport changes observed here have apparently both a wind-driven and a thermohaline (AMOC) component and both are difficult to account for. As noted earlier by Piecuch (2020) it appears difficult to establish a tight link between transport change and atmospheric forcing. The marginal decrease in AMOC strength reported here is probably associated with changes in the subpolar North Atlantic, since the outflow from the Nordic Seas shows no trend over the last 70 years (Rossby et al., 2020). On the other hand, a recent study (Chafik et al., 2022)

suggests a possible 2.2 Sv weakening of the subpolar AMOC over the last 70 years, but its significance remains unclear due to large interannual variations (variations that are not observed in the Nordic Seas overflow due to the large reservoir of the Nordic Seas acting as a low-pass filter). Thus, AMOC variability over the last 70–100 years appears to be tied to variations in the production of North Atlantic intermediate depth water.

We conclude by noting that so far as we know the subpolar AMOC remained active even during glacial times (Curry and Oppo, 2005) during which time overflow of dense water from the Nordic Seas was absent (e.g., Robinson et al., 2005). This reminds us that the AMOC equatorward return flow comprises two parts: what we might call North Atlantic Intermediate Water produced in the subpolar North Atlantic to at most 2 km depth (with entrainment to greater depths), and North Atlantic Deep Water, which slides into the deep North Atlantic from the Nordic Seas. The glacial—interglacial climate switches are associated with the state of the Nordic Seas, less so the subpolar North Atlantic.

Data Availability Statement

All data used here are publicly available and come from the EN4 archive: https://www.metoffice.gov.uk/hadobs/en4/.

References

Andres, M., Donohue, K. A., & Toole, J. M. (2020). The Gulf Stream's path and time-averaged velocity structure and transport at 68.5 W and 70.3 W. *Deep Sea Research Part I*, *156*, 103179. https://doi.org/10.1016/j.dsr.2019.103179

Bisagni, J. J., Gangopadhyay, A., & Sanchez-Franks, A. (2017). Secular change and inter-annual variability of the Gulf Stream position, 1993–2013, 70°−55°W. *Deep Sea Research Part I*, *125*, 1–10. https://doi.org/10.1016/j.dsr.2017.04.001

Caesar, L., McCarthy, G. D., Thornalley, D. J. R., Cahill, N., & Rahmstorf, S. (2021). Current Atlantic meridional overturning circulation weakest in last millennium. *Nature Geoscience*, *14*(3), 118–120. https://doi.org/10.1038/s41561-021-00699-z

Caesar, L., Rahmstorf, S., Robinson, A., Feulner, G., & Saba, V. (2018). Observed fingerprint of a weakening Atlantic Ocean overturning circulation. *Nature*, *556*(7700), 191–196. https://doi.org/10.1038/s41586-018-0006-5

Chafik, L., Holliday, N. P., Bacon, S., & Rossby, T. (2022). Irminger Sea is the center of action for subpolar AMOC variability. *Geophysical Research Letters*, *49*(17), e2022GL099133. https://doi.org/10.1029/2022GL099133

Chidichimo, M. P., Kanzow, T., Cunningham, S. A., Johns, W. E., & Marotzke, J. (2010). The contribution of eastern-boundary density variations to the Atlantic meridional overturning circulation at 26.5°N. *Ocean Science Discussions*, *6*(2), 475–490. https://doi.org/10.5194/os-6-475-2010. www.ocean-sci.net/6/475/2010/

Colin de Verdière, A., Meunier, T., & Ollitrault, M. (2019). Meridional overturning and heat transport from Argo floats displacements and the planetary geostrophic method (PGM): Application to the subpolar North Atlantic. *Journal of Geophysical Research: Oceans*, *124*(8), 6270–6285. https://doi.org/10.1029/2018JC014565

Compo, G. P., Whitaker, J. S., Sardeshmukh, P. D., Matsui, N., Allan, R. J., Yin, X., et al. (2011). The twentieth century reanalysis project. *Quarterly Journal of the Royal Meteorological Society*, *37*(654), 1–28. https://doi.org/10.1002/qj.776

Cunningham, S. A., Kanzow, T., Rayner, D., Baringer, M. O., Johns, W. E., Marotzke, J., et al. (2007). Temporal variability of the Atlantic Meridional overturning circulation at 26.5°N. *Science*, *317*(5840), 935–938. https://doi.org/10.1126/science.1141304

Curry, R. G., & McCartney, M. S. (2001). Ocean gyre circulation changes associated with the North Atlantic Oscillation. *Journal of Physical Oceanography*, *31*(12), 3374–3400. https://doi.org/10.1175/1520-0485(2001)031<3374:ogccaw>2.0.co;2

Curry, W. B., & Oppo, D. W. (2005). Glacial water mass geometry and the distribution of δ^{13}13C of ΣCO_2 in the western Atlantic Ocean. *Paleoceanography*, *20*(1), PA1017. https://doi.org/10.1029/2004PA001021

Danabasoglu, G., Yeager, S. G., Bailey, D., Behrens, E., Bentsen, M., Bi, D., et al. (2014). North Atlantic simulations in coordinated ocean-ice reference experiments phase II (CORE-II). Part I: Mean states. *Ocean Modelling*, *73*, 76–107. https://doi.org/10.1016/j.ocemod.2013.10.005

Ezer, T., & Dangendorf, S. (2020). Global sea level reconstruction for 1900–2015 reveals regional variability in ocean dynamics and an unprecedented long weakening in the Gulf Stream flow since the 1990s. *Ocean Science*, *16*(4), 997–1016. https://doi.org/10.5194/os-16-997-2020

Fofonoff, N. P. (1962). Dynamics of ocean currents. In M. N. Hill (Ed.), *Physical oceanography* (Vol. 1, pp. 323–395). John Wiley & Sons.

Fox-Kemper, B., Hewitt, H. T., Xiao, C., Aðalgeirsdóttir, G., Drijfhout, S. S., Edwards, T. L., et al. (2021). Ocean, cryosphere and sea level change. In V. Masson-Delmotte, P. Zhai, A. Pirani, S. L. Connors, C. Péan, S. Berger, et al. (Eds.), *Climate change 2021: The physical science basis. Contribution of working group I to the sixth assessment report of the intergovernmental panel on climate change*. Cambridge University Press. Retrieved from https://www.ipcc.ch/report/sixth-assessment-report-working-group-i/

Frajka-Williams, E., Moat, B. I., Smeed, D. A., Rayner, D., Johns, W. E., Baringer, M. O., et al. (2021). *Atlantic meridional overturning circulation observed by the RAPID-MOCHA-WBTS (RAPID-Meridional overturning circulation and heatflux array-western boundary time series) array at 26°N from 2004 to 2020 (v2020.1)*. British Oceanographic Data Centre—Natural Environment Research Council, UK. https://doi.org/10.5285/cc1e34b3-3385-662b-e053-6c86abc03444

Fraser, N. J., & Cunningham, S. A. (2021). 120 years of AMOC variability reconstructed from observations using the Bernoulli inverse. *Geophysical Research Letters*, *48*(18), e2021GL093893. https://doi.org/10.1029/2021gl093893

Gonçalves Neto, A., Langan, J. A., & Palter, J. B. (2021). Changes in the Gulf stream preceded rapid warming of the northwest Atlantic Shelf. *Communications Earth & Environment*, *2*(74), 74. https://doi.org/10.1038/s43247-021-00143-1

Helland-Hansen, B., & Nansen, F. (1909). The Norwegian sea, its physical oceanography based upon the Norwegian researches 1900-04. Report on Norwegian fishery and marine investigations, vol. II, Part I. Fiskeridirektoratet.

IPCC. (2021). IPCC. In V. Masson-Delmotte, P. Zhai, A. Pirani, S. L. Connors, C. Péan, et al. (Eds.), *Climate change 2021: The physical science basis. Contribution of working group I to the sixth assessment report of the intergovernmental panel on climate change*. Cambridge University Press. Retrieved from https://www.ipcc.ch/report/ar6/wg1/downloads/report/IPCC_AR6_WGI_SPM_final.pdf

Iselin, C. O. 'D. (1936). A study of the circulation of the Western North Atlantic. *Papers in Physical Oceanography and Meteorology*, *4*(4), 101.

Iselin, C. O. 'D. (1940). Preliminary report on long-period variations in the transport of the Gulf Stream system. *Papers in Physical Oceanography and Meteorology*, *8*(1), 40.

Joyce, T. M., & Robbins, P. (1996). The long-term hydrographic record at Bermuda. *Journal of Climate*, *9*(12), 3121–3131. https://doi.org/10.1175/1520-0442(1996)009<3121:tlthra>2.0.co;2

Kilbourne, K. H., Wanamaker, A. D., Moffa-Sanchez, P., Reynolds, D. J., Amrhein, D. E., Butler, P. G., et al. (2022). Atlantic circulation change still uncertain. *Nature Geoscience*, *15*(3), 165–167. https://doi.org/10.1038/s41561-022-00896-4

Little, C. M., Zhao, M., & Buckley, M. W. (2020). Do surface temperature indices reflect centennial-timescale trends in Atlantic Meridional Overturning Circulation strength? *Geophysical Research Letters*, *47*(22), e2020GL090888. https://doi.org/10.1029/2020GL090888

Lumpkin, R., & Speer, K. (2007). Global ocean meridional overturning. *Journal of Physical Oceanography*, *37*(10), 2550–2562. https://doi.org/10.1175/JPO3130.1

Menary, M. B., Robson, J., Allan, R. P., Booth, B. B. B., Cassou, C., Gastineau, G., et al. (2020). Aerosol-forced AMOC changes in CMIP6 historical simulations. *Geophysical Research Letters*, *47*(14), e2020GL088166. https://doi.org/10.1029/2020GL088166

Ollitrault, M., & de Verdière, A. C. (2014). The ocean general circulation near 1000-m depth. *Journal of Physical Oceanography*, *44*, 384–409.

Palter, J. B. (2015). The role of the Gulf Stream in European climate. *Annual Review of Marine Science*, *7*(1), 113–137. https://doi.org/10.1146/annurev-marine-010814-015656

Piecuch, C. G. (2020). Likely weakening of the Florida Current during the past century revealed by sea-level observations. *Nature Communications*, *11*(1), 3973. https://doi.org/10.1038/s41467-020-17761-w

Piecuch, C. G., Huybers, P., Hay, C. C., Kemp, A. C., Little, C. M., Mitrovica, J. X., et al. (2018). Origin of spatial variation in US East Coast sea-level trends during 1900–2017. *Nature*, *564*(7736), 400–404. https://doi.org/10.1038/s41586-018-0787-6

Poli, P., Hersbach, H., Dee, D. P., Berrisford, P., Simmons, A. J., Vitart, F., et al. (2016). ERA-20C: An atmospheric reanalysis of the twentieth century. *Journal of Climate*, *29*(11), 4083–4097. https://doi.org/10.1175/jcli-d-15-0556.1

Robinson, L. F., Adkins, J. F., Keigwin, L. D., Southon, J., Fernandez, D. P., & S-L WangScheirer, D. S. (2005). Radiocarbon variability in the western North Atlantic during the last deglaciation. *Science*, *310*(5753), 1469–1473. https://doi.org/10.1126/science.1114832

Rossby, T., Chafik, L., & Houpert, L. (2020). What can hydrography tell us about the strength of the Nordic Seas MOC over the last 70 to 100 years? *Geophysical Research Letters*, *47*(12), e2020GL087456. https://doi.org/10.1029/2020GL087456

Rossby, T., Flagg, C., Donohue, K., Fontana, S., Curry, R., Andres, M., & Forsyth, J. (2019). The Oleander is more than a flower: Twenty-five years of oceanography aboard a merchant vessel. *Oceanography*, *32*(3), 82–95.

Sato, O., & Rossby, T. (1995). Seasonal and secular variations in dynamic height anomaly and transport of the Gulf Stream. *Deep-Sea Research*, *42*(1), 149–164. https://doi.org/10.1016/0967-0637(94)00034-p

Stevens, S. W., Johnson, R. J., Maze, G., & Bates, N. R. (2020). A recent decline in North Atlantic subtropical mode water formation. *Nature Climate Change*, *10*(4), 335–341. https://doi.org/10.1038/s41558-020-0722-3

Sverdrup, H. U., Johnson, M. W., & Fleming, R. H. (1942). *The oceans, their physics, chemistry, and general biology*. Prentice-Hall. Retrieved from http://ark.cdlib.org/ark:/13030/kt167nb66r/

UNESCO. (1991). *Processing of oceanographic station data* (p. 138). JPOTS.

Wunsch, C. (2011). The decadal mean ocean circulation and Sverdrup balance. *Journal of Marine Research*, *69*(2), 417–434. https://doi.org/10.1357/002224011798765303

Yeager, S., Castruccio, F., Chang, P., Danabasoglu, G., Maroon, E., Small, J., et al. (2021). An outsized role for the Labrador Sea in the multidecadal variability of the Atlantic overturning circulation. *Science Advances*, *7*(41), eabh3592. https://doi.org/10.1126/sciadv.abh3592

Yin, J., & Goddard, P. B. (2013). Oceanic control of sea level rise patterns along the East Coast of the United States. *Geophysical Research Letters*, *40*(20), 5514–5520. https://doi.org/10.1002/2013GL057992

References From the Supporting Information

Isemer, H.-J., & Hasse, L. (1987). The bunker climate atlas of the North Atlantic Ocean. In *Air-Sea interactions* (Vol. 2, p. 255). Springer-Verlag.